Published in final edited form as:
Biochim Biophys Acta. 2013 August ; 1831(8): 1377–1385. doi:10.1016/j.bbalip.2013.04.013.

Intestinal acyl-CoA:diacylglycerol acyltransferase 2 overexpression enhances postprandial triglyceridemic response and exacerbates high fat diet-induced hepatic triacylglycerol storage

Aki Uchida[a,b], **Mikhail N. Slipchenko**[c], **Trisha Eustaquio**[c,d], **James F. Leary**[c,d,e], **Ji-Xin Cheng**[c,f], and **Kimberly K. Buhman**[a,b,*]

Kimberly K. Buhman: kbuhman@purdue.edu

[a]Interdisciplinary Life Science Program, Purdue University, West Lafayette, IN, USA

[b]Department of Nutrition Science, Purdue University, West Lafayette, IN, USA

[c]Weldon School of Biomedical Engineering, Purdue University, West Lafayette, IN, USA

[d]Birck Nanotechnology Center Purdue University, West Lafayette, IN, USA

[e]Department of Basic Medical Sciences, Purdue University, West Lafayette, IN, USA

[f]Department of Chemistry, Purdue University, West Lafayette, IN, USA

Abstract

Intestinal acyl-CoA:diacylglycerol acyltransferase 2 (DGAT2) is important in the cellular and physiological responses to dietary fat. To determine the effect of increased intestinal DGAT2 on cellular and physiological responses to acute and chronic dietary fat challenges, we generated mice with intestine-specific overexpression of DGAT2 and compared them with intestine-specific overexpression of DGAT1 and wild-type (WT) mice. We found that when intestinal DGAT2 is present in excess, triacylglycerol (TG) secretion from enterocytes is enhanced compared to WT mice; however, TG storage within enterocytes is similar compared to WT mice. We found that when intestinal DGAT2 is present in excess, mRNA levels of genes involved in fatty acid oxidation were reduced. This result suggests that reduced fatty acid oxidation may contribute to increased TG secretion by overexpression of DGAT2 in intestine. Furthermore, this enhanced supply of TG for secretion in Dgat2^{Int} mice may be a significant contributing factor to the elevated fasting plasma TG and exacerbated hepatic TG storage in response to a chronic HFD. These results highlight that altering fatty acid and TG metabolism within enterocytes has the capacity to alter systemic delivery of dietary fat and may serve as an effective target for preventing and treating metabolic diseases such as hepatic steatosis.

*Corresponding author at: Department of Nutrition Science, Purdue University, 700 W. State Street, West Lafayette, IN 47907, USA. Tel.: +1 765 496 6872; fax: +1 765 494 0674.

Supplementary data to this article can be found online at http://dx.doi.org/10.1016/j.bbalip.2013.04.013.

Keywords

Acyl-CoA:diacylglycerol acyltransferase; Chylomicron; Cytoplasmic lipid droplet; Dietary fat absorption; Triacylglycerol; Intestine

1. Introduction

When present in excess, dietary fat contributes to health problems including obesity, diabetes, heart disease, and hepatic steatosis. Dietary fat in excess can instigate health problems due to its high energy density and its impact on blood lipid concentrations. Dietary fat absorption is a highly efficient process with greater than 95% of dietary fat absorbed whether the diet is high or low in dietary fat [1]. Dietary fat, in the form of triacylglycerol (TG), is hydrolyzed in the intestinal lumen to monoacylglycerol and free fatty acids. These digestive products are then taken up by the absorptive cells of the intestine, enterocytes, and are primarily incorporated into TG either for secretion on TG-rich lipoproteins, chylomicrons (CM), or storage in cytoplasmic lipid droplets (CLDs) [2,3]. The storage and secretion of TG by enterocytes are dynamic and dose dependent processes. TG storage in CLDs within enterocytes and TG secretion from enterocytes initially increase and then decrease over time after a meal containing fat [2,4,5]. Recently, we and others have demonstrated that it is not only the amount of fat, but also the rate that dietary fat is delivered in blood to other tissues that contributes to some health problems associated with dietary fat [4,6]. Therefore, discerning the factors that regulate the balance between TG storage and secretion within enterocytes is critical to our mechanistic understanding of the contribution of dietary fat to these health problems.

The final and committed step in TG biosynthesis is the acylation of diacylglycerol with a fatty acid by acyl-CoA:diacylglycerol acyltransferase (DGAT). In mammals, there are two known, non-homologous proteins catalyzing DGAT activity: DGAT1 and DGAT2. DGAT1 and DGAT2 are both expressed ubiquitously; however, their relative tissue and cellular expression patterns are distinct [7,8]. Specifically, DGAT1 is most abundant in the small intestine, whereas DGAT2 is most abundant in adipose tissue and liver. In mouse intestine, the expression pattern of DGAT1 and DGAT2 is similar; highest in the proximal intestine and lowest in the distal intestine [8]. In human intestine, DGAT1 is abundant; however, DGAT2 may be present in much lower levels or even absent [9,10]; however, a thorough evaluation of DGAT2 expression in human enterocytes has not been done. Intracellularly, DGAT1 and DGAT2 both localize to the endoplasmic reticulum; however, DGAT2 has also been identified on CLDs [11,12] and in mitochondria associated membranes [12]. The ability to synthesize TG directly on CLDs contributes to the expansion of CLD size [11]. In addition to their different biochemical properties, these differences in expression patterns contribute to their different cellular and physiological functions [13,14].

In enterocytes, DGAT1 plays an important role in determining the balance between TG storage and secretion, and determining the systemic fate of dietary fat. Although *Dgat1*$^{-/-}$ mice quantitatively absorb dietary fat similarly to wild-type (WT) mice and can make CMs, their process of dietary fat absorption is altered. *Dgat1*$^{-/-}$ mice accumulate abnormally high levels of TG in CLDs within enterocytes when fed a high fat diet (HFD) and secrete TG

slowly compared to WT mice [8]. Similar results have also been reported in WT mice treated with DGAT1 inhibitors [15–18]. In addition, mice with intestine-specific overexpression of DGAT1 (*Dgat1*^{Int}) store abnormally low levels of TG within enterocytes when fed a HFD, but secrete TG at a similar rate compared with WT mice [4]. Finally, despite lacking DGAT1 in adipose tissue and liver, mice with DGAT1 expression only in the intestine (*Dgat1*^{Int} crossed with *Dgat1*$^{-/-}$ mice), are susceptible to HFD induced obesity and hepatic steatosis. Collectively, these results suggest that intestinal DGAT1 is not required for CM synthesis and secretion, but is important in the trafficking of dietary fat within enterocytes and systemically. These results also suggest that DGAT2 makes TG for storage and secretion in the absence of DGAT1, but the balance is altered. Clearly, DGAT1 and DGAT2 are working together in enterocytes to synthesize TG and mediate efficient dietary fat absorption.

The role of DGAT2 in intestine is less clear due to the fact that *Dgat2*$^{-/-}$ mice die shortly after birth [19]. DGAT2, but not DGAT1, mRNA levels in mouse intestinal mucosa increase in response to both acute and chronic HF dietary challenges [5]. In addition, DGAT2 mRNA levels in small intestine of obese and diabetic mouse strains (ob/ob, db/db and KK-A^{y}) are higher than in control mice [5,20,21]. To determine the effect of increased intestinal DGAT2 in the small intestine on cellular and physiological responses to acute dietary fat challenges and chronic HFD feeding, we generated mice with intestine-specific overexpression of DGAT2 (*Dgat2*^{Int}) and compared them with WT and *Dgat1*^{Int} mice. Although the basic phenotype of *Dgat1*^{Int} mice has previously been reported [4], we included *Dgat1*^{Int} mice in these experiments so we could compare high DGAT2/DGAT1 (*Dgat2*^{Int}), normal DGAT2/DGAT1 (WT), and low DGAT2/DGAT1 (*Dgat1*^{Int}) ratios in enterocytes on TG metabolism.

2. Materials and methods

2.1. Diets and mice

All procedures were approved by the Purdue Animal Care and Use Committee. The VILL-*Dgat2* transgene was made with a 12.4-kb VILL promoter/enhancer from the pUC12.4-kb-villin plasmid (Dr. Deborah L. Gumucio, University of Michigan, Ann Arbor, Michigan) and a 1.2-kb *Dgat2* cDNA sequence from the MDGAT2αF(MDC$_1$F)/pcDNA3 plasmid (Dr. Robert V. Farese Jr, Gladstone Institutes, San Francisco, California). The final transgene clone containing the villin promoter/enhancer and mouse *Dgat2* cDNA was verified by restriction mapping and sequence analysis. The transgene was prepared by digestion with PmeI and purification before introduction into C57BL/6 fertilized eggs by microinjection (Purdue Transgenic Core Facility, Purdue University, West Lafayette, Indiana). Founder animals were backcrossed with C57BL/6 mice to generate mice with intestine-specific overexpression of *Dgat2*. Two lines of mice with either 4- or 9-fold overexpression of *Dgat2* mRNA compared to WT were generated. Results presented are for the line with 4-fold overexpression of *Dgat2* mRNA levels compared to WT mice, and are referred to as *Dgat2*^{Int}. Similar results for the line with 9-fold overexpression of *Dgat2* mRNA levels compared to WT mice were found and are reported as *Dgat2*^{IntB} in the Supplementary data. Male *Dgat1*^{Int} mice (intestine-specific 20-fold overexpression of *Dgat1* mRNA level

compared to WT mice) were generated as previously described [4]. *Dgat1*^{Int} and *Dgat2*^{Int} were crossed with *Dgat1*$^{-/-}$ mice to generate *Dgat1*$^{-/-}$*Dgat1*^{Int} and *Dgat1*$^{-/-}$*Dgat2*^{Int} mice.

All mice enrolled in the studies described were male and maintained in a specific pathogen-free barrier facility with a 12-hour light/dark cycle (6AM/6PM). Mice were fed, either a low-fat, rodent chow diet (PicoLab 5053, Lab Diets, Richmond, IN), or a HFD (D12492, Research Diets, Inc., New Brunswick, NJ) for the indicated times. For chow diet (3.4 kcal/g), 62.1% of calories came from carbohydrate (starch), 24.7% from protein, and 13.2% from fat. For HFD (5.24 kcal/g), 20% of calories came from carbohydrate (35% sucrose, 65% starch), 20% from protein, and 60% from fat (mostly lard). Mice were enrolled in body weight studies at 10 weeks of age and fed indicated diets for 9 weeks. Mice not enrolled in body weight studies were 3–5 months of age and fed indicated diets.

Mice were euthanized and tissues harvested at specific time points relative to the fed-fasted cycle. *Fed*: For mice representing the fed state, food was removed at the beginning of the light cycle (6AM) and mice were euthanized at 8AM. The 2 h of food removal was at a time period where mice are normally not eating and was intended to minimize the variability in time since last food consumption. *Time course*: For the time course, all mice had food removed for 4 h prior to a 200 μl olive oil gavage and were euthanized at baseline, and 1, 2, 4, or 8 h post-gavage. After administration of the olive oil gavage, no other food was available during the time course. For analysis, we divided the small intestine into six equal-length segments and labeled them S1–S6 (proximal to distal). We scraped mucosa from each region of the intestine for RT-PCR, QPCR, and intestinal TG quantification.

2.2. Genotyping

Genotyping for *Dgat2*^{Int} was performed on genomic DNA extracted from tails to determine the presence or absence of transgene and/or endogenous gene. Primer sets Forward 5′-GAGTGGCCTGCAGTGTCATCC-3′ and Reverse 5′-GGATGGGAAAGTAGTCTCGGAAGTAGC-3′ were used to detect the presence of a transgene, amplifying a 177 bp product in transgenic mice and 505 bp product in WT mice. Genotyping for *Dgat1*^{Int} and *Dgat1*$^{-/-}$ mice was performed as previously described [4].

2.3. Fasting plasma TG and glucose concentration

Mice were fasted for 12 h, and blood samples were obtained from the submandibular vein. TG concentration was determined by Wako L-Type TG determination kit (Wako Chemicals USA) and glucose concentration was determined by OneTouch glucometer (LifeScan, Milpitas, CA).

2.4. Postprandial triglyceridemic response

Mice were fasted for 4 h starting at the beginning of the light cycle, and administered an oral gavage of 200 μl olive oil and blood collected via submandibular vein up to 4 h post-gavage. Plasma TG concentration was determined by Wako L-Type TG determination kit (Wako Chemicals USA, Richmond, VA).

2.5. Hepatic and intestinal TG secretion

Mice were fasted for 4 h starting at the beginning of the light cycle and administered 500 mg/kg Tyloxapol (T0307, Sigma-Aldrich, St. Louis, MO) via IP injection to block lipase activity in circulation. For hepatic TG secretion, blood was collected from the submandibular vein 1, 2 and 4 h post Tyloxapol injection. For intestinal TG secretion, 30 min post-Tyloxapol injection, mice were given 200 μl olive oil via oral gavage and blood collected via the submandibular vein 2 and 4 h post-gavage. Plasma TG concentration was determined by Wako L-Type TG determination kit (Wako Chemicals USA).

2.6. CM size

CMs were isolated from plasma collected 1 h post 200 μl olive oil oral gavage. Briefly, PBS was layered on to 50 μl plasma in a 230 μl polycarbonate thickwall ultracentrifuge tube and spun for 30 min at 50,000 ×g in a bench top ultracentrifuge (Optima Max XP, Beckman Coulter, Brea, CA) and the top layer collected. Dynamic light scattering (DLS) was used to measure hydrodynamic diameter of CMs. DLS measurements (three repeated measurements per sample) were taken at room temperature using the automatic mode on the Zetasizer Nano ZS (Malvern Instruments, Worcestershire, UK) to choose the appropriate settings for run length and number of runs per measurement. The Z averages, dominant intensity peak, and polydispersity indices are reported. The Z average is the intensity weighted mean hydrodynamic size of the entire population of CMs. The dominant intensity peak indicates only the most prominent chylomicron population. The polydispersity index is related to the standard deviation of the hypothetical Gaussian distribution of particle size. Both are derived from cumulant analysis of the DLS measured intensity autocorrelation function [5,22,23].

2.7. Dietary fat absorption

In singly housed cages, food intake was determined over 5 days and feces were collected daily. The feces were dried for 2 h in an ANKOMRD dryer (ANKOM Technology, Macedon, NY) and then lipids were extracted by automated Soxhlet extraction (petroleum ether) using the ANKOM^{XT15} extraction system (ANKOM Technology). The analysis is achieved by measuring the loss of mass due to the extraction of fat from the dried fecal samples.

2.8. Intestinal and liver TG concentrations

Lipids in intestinal mucosa (S2 and S3, representing jejunum) and liver were extracted by the hexane/isopropanol method. Briefly, after homogenization of the mucosa with 1 M Tris–HCL (pH 7.4), hexane/isopropanol (3:2) and water were added to the sample and it was incubated for 30 min with occasional mixing. The upper organic layer was evaporated under nitrogen and lipids were dissolved in isopropanol. TG concentration was determined by Wako L-Type TG determination kit (Wako Chemicals USA) and normalized to protein concentration (Pierce, Rockford, IL).

2.9. Tissue imaging

For intact tissue imaging, ex vivo fresh tissues from small intestine (S2, representing upper jejunum, and S4, representing lower jejunum) were placed in 3 ml Dulbecco's Modified

Eagle's Medium (Gibco, Carlsbad, CA) supplemented with 20 mM HEPES, 100 U/ml penicillin–streptomycin (Gibco), and 10% fetal bovine serum. Tissues kept at 4 °C maintained good morphology over 5 h. Small intestine tissue was cut longitudinally and laid flat for luminal imaging. All tissues were imaged within 3 h after euthanasia. Coherent anti-Stokes Raman scattering (CARS) imaging was performed using a multimodal microscope as previously described [5].

2.10. RT-PCR and QPCR

Total RNA was extracted from tissues with RNA STAT60 (Tel-Test, Friendswood, TX) and then DNase treated with Turbo DNA-free (Ambion, Austin, TX). cDNA was synthesized from 1 μg DNase treated RNA by AffinityScript qPCR cDNA using oligo dT and random hexamer primers (Stratagene, La Jolla, CA). QPCR and RT-PCR were performed using Mx3000P QPCR System (Stratagene) and Brilliant SYBR green master mix (Stratagene) or GoTaq Green master mix (Promega, Madison, WI), respectively. The expression of each gene was normalized to 18S rRNA and calculated with the comparative Ct method. For determination of tissue-specific transgene expression in *Dgat2*^{Int} mice, a primer sequence partially upstream of the *Dgat2* transgene, Forward 5′-CTTCTCCTCTAGGCTCGTCCACCC-3′, and the reverse primer within the transgene, Reverse 5′-TCTTGGGCGTGTTCCAGTCAAATG-3′, were used for RT-PCR. QPCR primers used for this study were all validated for efficiency and correct product size in cDNA from mouse intestinal mucosa (Table 1).

2.11. Data and statistics

All the data are shown as mean ± SEM. Statistical differences were evaluated with one-way ANOVA followed by a Tukey HSD test between groups, or a *T-test* where appropriate ($P < 0.05$).

3. Results

3.1. Generation of mice overexpressing mouse *Dgat2* in the intestine (*Dgat2*^{Int})

Dgat2^{Int} mice were generated with a DNA construct containing the villin promoter/enhancer driving the expression of mouse *Dgat2* (Fig. 1A). The villin promoter/enhancer drives expression in epithelial cells of the small and large intestine as well as from crypt to tip on the villus beginning as early as 12.5 dpc [24]. We generated mice with 4-fold (*Dgat2*^{Int}) and 9-fold (*Dgat2*^{IntB}, Supplementary data) overexpression of *Dgat2* mRNA levels compared to WT mice fed a low fat, chow diet determined by QPCR. Using RT-PCR, we determined that the transgene was present along the length of the small intestine, colon, and kidney but not in muscle, liver and adipose tissue (Fig. 1B). Using QPCR we found that *Dgat2* mRNA levels were only elevated in the small intestine and colon of *Dgat2*^{Int} mice and not in kidney, muscle, liver or adipose tissue (Fig. 1C). *Dgat1* mRNA levels were similar in the jejunum of WT and *Dgat2*^{Int} mice (Fig. 1D).

A group of *Dgat2*^{Int} and WT littermate controls were weaned at 3 weeks of age to a chow diet and weighed weekly until 18 weeks of age. *Dgat2*^{Int} and WT littermate controls had similar body weight curves, liver and gonadal fat pad weights as well as fasting blood

glucose and TG concentrations (Fig. 2A, C and D). A subgroup of *Dgat2*^{Int} and WT littermate controls were switched to a HFD for 9 weeks at 10 weeks of age. Likewise, *Dgat2*^{Int} and WT littermate controls fed HFD had similar body weights throughout the study (Fig. 2B). In addition, liver weights, gonadal fat pad weights, fasting plasma glucose concentrations, and dietary fat absorption were similar at the end of the study in *Dgat2*^{Int} and WT littermate controls fed HFD (Fig. 2C and Table 2). Interestingly, we found increased fasting plasma TG concentration in *Dgat2*^{Int} compared to WT littermate controls fed HFD (Fig. 2D).

3.2. Metabolic characterizations of male *Dgat1*^{Int} mice

We found that male *Dgat1*^{Int} mice, fed chow or HFD, have similar body weight curves, liver and gonadal fat pad weight as well as fasting plasma glucose and TG concentrations compared to WT mice (Fig. 3A–D). Likewise, food intake and dietary fat absorption were similar between *Dgat1*^{Int} and WT littermate mice fed HFD (Table 2). These results were similar to previously reported data in female *Dgat1*^{Int} mice [4].

3.3. Increased postprandial triglyceridemic response and intestinal TG secretion, but similar liver TG secretion, in chow-fed *Dgat2*^{Int} compared to *Dgat1*^{Int} and WT mice

To determine whether increased intestinal expression of *Dgat1* or *Dgat2* alters postprandial triglyceridemic response, we measured plasma TG concentrations hourly for up to 4 h post-acute dietary fat challenge in *Dgat1*^{Int}, *Dgat2*^{Int} and WT mice fed a chow diet. We found a greater postprandial triglyceridemic response as determined by increased area under the curve in *Dgat2*^{Int} compared to *Dgat1*^{Int} and WT mice (Fig. 4A). To determine whether the greater postprandial triglyceridemic response in *Dgat2*^{Int} mice was due to an increase in intestinal TG secretion, we measured plasma TG concentration before and at 2 and 4 h post-acute dietary fat challenge in TG clearance inhibitor, Tyloxapol, treated *Dgat1*^{Int}, *Dgat2*^{Int} and WT mice. We found that *Dgat2*^{Int} mice have increased TG secretion from enterocytes as evidenced by a faster rate of TG accumulation in the plasma during the 4-hour time course (Fig. 4B).

To confirm that the difference in TG secretion rates after an acute dietary fat challenge is due to the contribution from the small intestine and not the liver, we measured plasma TG concentrations at 0, 1, 2 and 4 h post Tyloxapol injection in *Dgat1*^{Int}, *Dgat2*^{Int} and WT mice. We found similar rates of TG accumulation in the plasma of *Dgat1*^{Int}, *Dgat2*^{Int} and WT mice (Fig. 4C).

In addition, to determine whether CM size was altered in *Dgat1*^{Int} and *Dgat2*^{Int} mice, we isolated CMs via ultracentrifugation 1 h post-acute dietary fat challenge and measured their size via DLS. We found that CMs isolated from the *Dgat1*^{Int} and *Dgat2*^{Int} mice were similar in size compared to WT mice (Table 3).

3.4. Decreased intestinal TG storage under chronic HF feeding and in response to an acute dietary fat challenge in *Dgat1*^{Int} compared to *Dgat2*^{Int} and WT mice

To determine whether increased intestinal expression of *Dgat1* or *Dgat2* altered TG storage in response to chronic HF feeding, we visualized TG storage via CARS microscopy in the

upper jejunum of *Dgat1*^{Int}, *Dgat2*^{Int} and WT mice fed a HFD for 9 weeks. Similar to previously published results in female, HF-fed *Dgat1*^{Int} mice [4], male, HF-fed *Dgat1*^{Int} mice had less TG storage in enterocytes than WT controls (Fig. 5A). Although not statistically significant, biochemical TG analysis resulted in similar trends of lower TG concentration in the jejunum of HF-fed *Dgat1*^{Int} mice compared to WT mice (Fig. 5B). We found that HF-fed *Dgat2*^{Int} mice did not have differential intestinal TG storage compared to WT mice (Fig. 5A and C).

To determine whether increased intestinal expression of *Dgat1* or *Dgat2* altered TG storage in response to an acute dietary fat challenge, we visualized TG storage via CARS microscopy in the upper jejunum of chow-fed *Dgat1*^{Int}, *Dgat2*^{Int} and WT mice at 1, 2, 4 and 8 h post-acute dietary fat challenge. We found that intestine-specific overexpression of *Dgat1* resulted in less TG storage in enterocytes, whereas intestine-specific overexpression of *Dgat2* did not result in differential TG storage in enterocytes in response to an acute dietary fat challenge compared to WT mice (Fig. 5D). We found similar results in the lower jejunum of chow-fed *Dgat1*^{Int}, *Dgat2*^{Int} and WT mice at 1, 2, 4 and 8 h post-acute dietary fat challenge (data not shown).

3.5. Decreased mRNA levels for genes involved in fatty acid oxidation under HF feeding in *Dgat2*^{Int} compared to *Dgat1*^{Int} and WT mice

We initially predicted that if TG secretion increases then TG storage would decrease and vice versa. However, in *Dgat2*^{Int} mice TG secretion increased and storage stayed the same. In *Dgat1*^{Int} mice, TG storage decreased and secretion stayed the same. Another fate of fatty acids in enterocytes is oxidation [25–27]. To determine whether increased intestinal expression of *Dgat1* or *Dgat2* may alter fatty acid oxidation in enterocytes, mRNA levels of genes involved in fatty acid oxidation were determined in jejunum of chronic HF-fed *Dgat1*^{Int}, *Dgat2*^{Int} and WT mice. We measured mRNA levels of (*Pparα*), acyl-CoA oxidase (Acox), carnitine palmitoyltransferase 1a (*Cpt1a*), fatty acid binding protein 2 (*Fabp2*), medium chain acyl-CoA dehydrogenase (*Acadm*), and long chain acyl-CoA dehydrogenase (*Acadl*). We found remarkably lower mRNA levels of *Pparα*, *Acox*, *Cpt1a*, *Fabp2*, and *Acadl* in the jejunum of HF-fed *Dgat2*^{Int} compared to *Dgat1*^{Int} and WT mice (Fig. 6).

3.6. Increased hepatic TG storage in HF-fed *Dgat2*^{Int} mice compared to WT and *Dgat1*^{Int} mice

To determine whether increased intestinal expression of *Dgat1* or *Dgat2* resulted in a susceptibility to HFD-induced hepatic steatosis, we fed *Dgat1*^{Int} and *Dgat2*^{Int} mice and WT littermates a HFD for 9 weeks. Despite the liver weights being similar between *Dgat2*^{Int} and WT mice, hepatic TG concentrations were significantly higher in *Dgat2*^{Int} compared to WT mice fed a HFD (Fig. 7B). We did not find significant differences in liver weights or hepatic TG concentrations in *Dgat1*^{Int} compared to WT mice fed a HFD (Fig. 7A). Similar hepatic TG concentrations were observed in chow-fed *Dgat1*^{Int} and *Dgat2*^{Int} mice and corresponding WT littermates (data not shown).

3.7. Abnormal intestinal TG accumulation in *Dgat1*$^{-/-}$ mice is reversed when crossed with *Dgat1*^{Int}, but not *Dgat2*^{Int} mice

To determine the specificity of DGAT1 and DGAT2 in intestinal TG metabolism, we imaged the upper jejunum of HFD-fed *Dgat1*$^{-/-}$, *Dgat1*$^{-/-}$*Dgat1*^{Int}, and *Dgat1*$^{-/-}$*Dgat2*^{Int} mice using CARS microscopy. We found that intestinal overexpression of *Dgat1*, but not *Dgat2* in *Dgat1*$^{-/-}$ mice corrected the abnormal intestinal TG accumulation of HFD-fed *Dgat1*$^{-/-}$ mice (Fig. 8). In addition, we characterized CM size of *Dgat1*$^{-/-}$ mice and found that the CM size in *Dgat1*$^{-/-}$ is significantly smaller compared to WT mice (Table 3).

4. Discussion

Intestinal DGAT2 is important in the cellular and physiological responses to dietary fat. We found that when the ratio of DGAT2/DGAT1 is high in enterocytes (*Dgat2*^{Int}), TG secretion from enterocytes is enhanced; however, TG storage within enterocytes is similar compared to WT mice. Furthermore, we determined that a high DGAT2/DGAT1 ratio in enterocytes resulted in reduced mRNA levels of genes involved in fatty acid oxidation, suggesting that the enhanced supply of TG for secretion may in part be due to reduced fatty acid oxidation. Ultimately, this enhanced supply of TG for secretion in *Dgat2*^{Int} mice may be a significant contributing factor to the elevated fasting plasma TG and increased hepatic TG stores in response to chronic HFD feeding.

We have confirmed that when present in the absence of DGAT1 (*Dgat1*$^{-/-}$), intestinal DGAT2 contributes to the synthesis of TG for secretion, but the size of the CMs is smaller and rate of TG secretion dramatically reduced, resulting in abnormal TG storage within enterocytes. We further confirmed that when intestinal DGAT2 is present with excess DGAT1 (*Dgat1*^{Int}), TG secretion from enterocytes is normal, but TG storage within enterocytes is reduced and the CLDs present appear smaller. Importantly, in all of these mouse models dietary fat absorption remained highly efficient and quantitatively similar. These results highlight that altering fatty acid and TG metabolism within enterocytes, without affecting quantitative dietary fat absorption, has the capacity to alter the systemic trafficking of dietary fat and may serve as an effective target for preventing and treating metabolic diseases such as hepatic steatosis.

Intestinal DGAT1 and DGAT2 contribute to TG synthesis for both storage and secretion. DGAT activity is primarily located in the endoplasmic reticulum (ER) of cells and has been characterized on both the cytosolic and lumenal sides of the ER membrane, referred to as overt and latent activities, respectively [28,29]. The concept of overt and latent DGAT activities proposes that TGs synthesized on the cytosolic side are destined for storage in CLDs, whereas TGs synthesized within the ER lumen are packaged for secretion on TG rich lipoproteins [30]. With the identification of two separate genes catalyzing DGAT activity, DGAT1 and DGAT2, the hypothesis that these two different proteins may be responsible for the synthesis of TG on separate sides of the ER membrane was proposed. In fact, initial topology studies of DGAT1 and DGAT2 were consistent with this idea with the active site of DGAT1 on the luminal side of the ER membrane [31,32] and the active site of DGAT2 on the cytosolic side of the ER membrane [33]. In addition to the data presented here, several pieces of evidence are inconsistent with a specific role of DGAT1 in synthesizing

TG for secretion and DGAT2 in synthesizing TG for storage. First, cell types without the ability to secrete TG on lipoproteins express both DGAT1 and DGAT2 [7]. Second, overexpression of DGAT1 or DGAT2 in cells without endogenous DGAT activity results in increased TG storage in CLDs [19]. Third, more recent topology studies suggest that DGAT1 may insert into the ER membrane with at least two different topologies with the active site on either side of the ER membrane [34]. Although altering relative levels of DGAT1 and DGAT2 in enterocytes changes the balance between TG storage and secretion as shown here, fatty acid supply and other proteins likely contribute in determining the fate of newly synthesized TGs.

One factor that may play a role in determining the fate of newly synthesized TG in cells is the cellular localization of DGAT2. In addition to the ER, DGAT2 protein and activity are associated with mitochondria associated membranes, mitochondria, and cytoplasmic lipid droplets [11,35]. Although the studies presented here did not specifically identify the cellular location of overexpressed DGAT2, we found remarkably lower mRNA levels of genes related to fatty acid oxidation in intestinal mucosa of HFD-fed *Dgat2*$^{\mathrm{Int}}$ compared to WT mice (Fig. 6). These results are consistent with our recently reported results in diet-induced obese mice where we found higher DGAT2 mRNA levels and a significant, and reduced PPARα mRNA level 2 h after a high fat challenge compared to lean mice [5]. Although levels of fatty acid oxidation in the intestine are considered low in comparison to other tissues [36,37], changes in intestinal fatty acid oxidation may alter fatty acid availability for TG synthesis and ultimately storage and secretion. In fact, dietary polyunsaturated fatty acids increase fatty acid oxidation in the intestine via a PPARα-dependent manner [25,38,39]. Furthermore, fibrate drugs, which are PPARα agonists, increase fatty acid oxidation in the small intestine and decrease the postprandial triglyceridemic response [26,40]. In *Dgat2*$^{\mathrm{Int}}$ mice, we found reduced PPARα mRNA levels, allowing us to speculate that intestinal DGAT2 plays a role in limiting fatty acid oxidation in enterocytes by localizing to the mitochondria or mitochondria associated membranes where it may channel fatty acids away from oxidation toward TG synthesis, CM secretion and eventually increased hepatic TG storage.

DGAT1 and DGAT2 work together with complementary, but not redundant, functions in processing dietary fat by the intestine. In the absence of DGAT1, DGAT2 is able to ensure quantitative absorption of dietary fat, but in this study we found that the CMs that are made are significantly smaller than CMs made in mice with both DGAT1 and DGAT2 (Table 3). We previously demonstrated that crossing *Dgat1*$^{-/-}$ and *Dgat1*$^{\mathrm{Int}}$ mice restores the intestine phenotype of *Dgat1*$^{-/-}$ mice including the abnormal TG storage and reduced rate of TG secretion. In addition, it restores their susceptibility to diet induced obesity and hepatic steatosis. We were curious whether adding more DGAT2 to enterocytes of *Dgat1*$^{-/-}$ mice may also complement this intestinal phenotype due to overall more DGAT activity. However, when we crossed *Dgat1*$^{-/-}$ and *Dgat2*$^{\mathrm{Int}}$ the abnormal TG storage phenotype remained (Fig. 8).

It is important to highlight that *Dgat1*$^{\mathrm{Int}}$ and *Dgat2*$^{\mathrm{Int}}$ mice retain endogenous DGAT1 and DGAT2 and thus these models only tip the balance of contribution of either DGAT1 or DGAT2 toward TG synthesis. Looking beyond the intestine, we found it particularly

interesting that increasing the contribution of DGAT2 in the intestine resulted in an increase in hepatic TG storage, since we and others have found that intestinal levels of DGAT2 are higher in genetic and diet-induced obesity models which have hepatic steatosis [5,20,21]. In summary, our results demonstrate that DGAT1 and DGAT2 work together to govern the number and size of CMs for TG secretion. In addition, our previous results suggest that DGAT1 and DGAT2 also govern the size of CLD for TG storage [11]. The different cellular and physiological responses to dietary fat challenges in these mouse models emphasize the distinct roles of these proteins and highlight that the relative levels of intestinal DGAT1 and DGAT2 are likely important in determining the response to dietary fat including regulation of postprandial blood TG levels as well as the development of HFD-induced hepatic steatosis.

Supplementary Material

Refer to Web version on PubMed Central for supplementary material.

Acknowledgments

This work was supported by AHA NCRP Scientist Development Grant 0835203 N to KKB, NIH R01EB7243 to JXC and AHA Predoctoral Fellowship 11PRE5140017 to AU.

References

1. Carey MC, Small DM, Bliss CM. Lipid digestion and absorption. Annu Rev Physiol. 1983; 45:651–677. [PubMed: 6342528]
2. Zhu JB, Lee BG, Buhman KK, Cheng JX. A dynamic, cytoplasmic triacylglycerol pool in enterocytes revealed by ex vivo and in vivo coherent anti-Stokes Raman scattering imaging. J Lipid Res. 2009; 50:1080–1089. [PubMed: 19218555]
3. Robertson MD, Parkes M, Warren BF, Ferguson DJP, Jackson KG, Jewell DP, Frayn KN. Mobilisation of enterocyte fat stores by oral glucose in humans. Gut. 2003; 52:834–839. [PubMed: 12740339]
4. Lee B, Fast AM, Zhu J, Chen JX, Buhman KK. Intestine specific expression of acyl CoA:diacylgylcerol acyltransferase 1 (DGAT1) reverses resistance to diet-induced hepatic steatosis and obesity in Dgat1$^{-/-}$ mice. J Lipid Res. 2010; 51:1770–1780. [PubMed: 20147738]
5. Uchida A, Whitsitt MC, Eustaquio T, Slipchenko MN, Leary JF, Cheng JX, Buhman KK. Reduced triglyceride secretion in response to an acute dietary fat challenge in obese compared to lean mice. Front Physiol. 2012; 3:26. [PubMed: 22375122]
6. Yen CLE, Cheong ML, Grueter C, Zhou P, Moriwaki J, Wong JS, Hubbard B, Marmor S, Farese RV. Deficiency of the intestinal enzyme acyl CoA:monoacylglycerol acyltransferase-2 protects mice from metabolic disorders induced by high-fat feeding. Nat Med. 2009; 15:442–446. [PubMed: 19287392]
7. Cases S, Smith SJ, Zheng YW, Myers HM, Lear SR, Sande E, Novak S, Collins C, Welch CB, Lusis AJ, Erickson SK, Farese RV Jr. Identification of a gene encoding an acyl CoA:diacylglycerol acyltransferase, a key enzyme in triacylglycerol synthesis. Proc Natl Acad Sci U S A. 1998; 95:13018–13023. [PubMed: 9789033]
8. Buhman KK, Smith SJ, Stone SJ, Repa JJ, Wong JS, Knapp FF, Burri BJ, Hamilton RL, Abumrad NA, Farese RV. DGAT1 is not essential for intestinal triacylglycerol absorption or chylomicron synthesis. J Biol Chem. 2002; 277:25474–25479. [PubMed: 11959864]
9. Cases S, Stone SJ, Zhou P, Yen E, Tow B, Lardizabal KD, Voelker T, Farese RV. Cloning of DGAT2, a second mammalian diacylglycerol acyltransferase, and related family members. J Biol Chem. 2001; 276:38870–38876. [PubMed: 11481335]

10. Haas JT, Winter HS, Lim E, Kirby A, Blumenstiel B, DeFelice M, Gabriel S, Jalas C, Branski D, Grueter CA, Toporovski MS, Walther TC, Daly MJ, Farese RV Jr. DGAT1 mutation is linked to a congenital diarrheal disorder. J Clin Invest. 2012; 122:4680–4684. [PubMed: 23114594]
11. Wilfling F, Wang H, Haas JT, Krahmer N, Gould TJ, Uchida A, Cheng JX, Graham M, Christiano R, Frohlich F, Liu X, Buhman KK, Coleman RA, Bewersdorf J, Farese RV Jr, Walther TC. Triacylglycerol synthesis enzymes mediate lipid droplet growth by relocalizing from the ER to lipid droplets. Dev Cell. 2013; 24:384–399. [PubMed: 23415954]
12. Stone SJ, Levin MC, Zhou P, Han JY, Walther TC, Farese RV. The endoplasmic reticulum enzyme DGAT2 is found in mitochondria-associated membranes and has a mitochondrial targeting signal that promotes its association with mitochondria. J Biol Chem. 2009; 284:5352–5361. [PubMed: 19049983]
13. Yen CL, Stone SJ, Koliwad S, Harris C, Farese RV Jr. Thematic review series: glycerolipids. DGAT enzymes and triacylglycerol biosynthesis. J Lipid Res. 2008; 49:2283–2301. [PubMed: 18757836]
14. Liu Q, Siloto RM, Lehner R, Stone SJ, Weselake RJ. Acyl-CoA:diacylglycerol acyltransferase: molecular biology, biochemistry and biotechnology. Prog Lipid Res. 2012; 51:350–377. [PubMed: 22705711]
15. Dow RL, Li JC, Pence MP, Gibbs EM, LaPerle JL, Litchfield J, Piotrowski DW, Munchhof MJ, Manion TB, Zavadoski WJ, Walker GS, McPherson RK, Tapley S, Sugarman E, Guzman-Perez A, DaSilva-Jardine P. Discovery of PF-04620110, a potent, selective, and orally bioavailable inhibitor of DGAT-1. ACS Med Chem Lett. 2011; 2:407–412. [PubMed: 24900321]
16. Cheng D, Iqbal J, Devenny J, Chu CH, Chen LP, Dong J, Seethala R, Keim WJ, Azzara AV, Lawrence RM, Pelleymounter MA, Hussain MM. Acylation of acylglycerols by acyl coenzyme A:diacylglycerol acyltransferase 1 (DGAT1) functional importance of DGAT1 in intestinal fat absorption. J Biol Chem. 2008; 283:29802–29811. [PubMed: 18768481]
17. Jadhav RD, Kadam KS, Kandre S, Guha T, Reddy MM, Brahma MK, Deshmukh NJ, Dixit A, Doshi L, Potdar N, Enose AA, Vishwakarma RA, Sivaramakrishnan H, Srinivasan S, Nemmani KV, Gupte A, Gangopadhyay AK, Sharma R. Synthesis and biological evaluation of isoxazole, oxazole, and oxadiazole containing heteroaryl analogs of biaryl ureas as DGAT1 inhibitors. Eur J Med Chem. 2012; 54:324–342. [PubMed: 22683241]
18. Yeh VS, Beno DW, Brodjian S, Brune ME, Cullen SC, Dayton BD, Dhaon MK, Falls HD, Gao J, Grihalde N, Hajduk P, Hansen TM, Judd AS, King AJ, Klix RC, Larson KJ, Lau YY, Marsh KC, Mittelstadt SW, Plata D, Rozema MJ, Segreti JA, Stoner EJ, Voorbach MJ, Wang X, Xin X, Zhao G, Collins CA, Cox BF, Reilly RM, Kym PR, Souers AJ. Identification and preliminary characterization of a potent, safe, and orally efficacious inhibitor of acyl-CoA:diacylglycerol acyltransferase 1. J Med Chem. 2012; 55:1751–1757. [PubMed: 22263872]
19. Stone SJ, Myers HM, Watkins SM, Brown BE, Feingold KR, Elias PM, Farese RV. Lipopenia and skin barrier abnormalities in DGAT2-deficient mice. J Biol Chem. 2004; 279:11767–11776. [PubMed: 14668353]
20. Douglass JD, Malik N, Chon SH, Wells K, Zhou YX, Choi AS, Joseph LB, Storch J. Intestinal mucosal triacylglycerol accumulation secondary to decreased lipid secretion in obese and high fat fed mice. Front Physiol. 2012; 3:25. [PubMed: 22375121]
21. Wakimoto K, Chiba H, Michibata H, Seishima M, Kawasaki S, Okubo K, Mitsui H, Torii H, Imai Y. A novel diacylglycerol acyltransferase (DGAT2) is decreased in human psoriatic skin and increased in diabetic mice, Biochem. Biophys Res Commun. 2003; 310:296–302.
22. Werner A, Havinga R, Perton F, Kuipers F, Verkade HJ. Lymphatic chylomicron size is inversely related to biliary phospholipid secretion in mice. Am J Physiol Gastrointest Liver Physiol. 2006; 290:G1177–G1185. [PubMed: 16384875]
23. Sakurai T, Trirongjitmoah S, Nishibata Y, Namita T, Tsuji M, Hui SP, Jin S, Shimizu K, Chiba H. Measurement of lipoprotein particle sizes using dynamic light scattering. Ann Clin Biochem. 2010; 47:476–481. [PubMed: 20736248]
24. Madison BB, Dunbar L, Qiao XT, Braunstein K, Braunstein E, Gumucio DL. Cis elements of the villin gene control expression in restricted domains of the vertical (crypt) and horizontal (duodenum, cecum) axes of the intestine. J Biol Chem. 2002; 277:33275–33283. [PubMed: 12065599]

25. van Schothorst EM, Flachs P, Hal NL Franssen-van, Kuda O, Bunschoten A, Molthoff J, Vink C, Hooiveld GJ, Kopecky J, Keijer J. Induction of lipid oxidation by polyunsaturated fatty acids of marine origin in small intestine of mice fed a high-fat diet. BMC Genomics. 2009; 10:110. [PubMed: 19284886]
26. Uchida A, Slipchenko MN, Cheng JX, Buhman KK. Fenofibrate, a peroxisome proliferator-activated receptor a agonist, alters triglyceride metabolism in enterocytes of mice. Biochim Biophys Acta, Mol Cell Biol Lipids. 2011; 1811:170–176.
27. Storch J, Zhou YX, Lagakos WS. Metabolism of apical versus basolateral sn-2-monoacylglycerol and fatty acids in rodent small intestine. J Lipid Res. 2008; 49:1762–1769. [PubMed: 18421071]
28. Owen M, Zammit VA. Evidence for overt and latent forms of DGAT in rat liver microsomes. Implications for the pathways of triacylglycerol incorporation into VLDL. Biochem Soc Trans. 1997; 25:21S. [PubMed: 9056919]
29. Owen MR, Corstorphine CC, Zammit VA. Overt and latent activities of diacylglycerol acytransferase in rat liver microsomes: possible roles in very-low-density lipoprotein triacylglycerol secretion. Biochem J. 1997; 323:17–21. Pt 1. [PubMed: 9173878]
30. Sturley SL, Hussain MM. Lipid droplet formation on opposing sides of the endoplasmic reticulum. J Lipid Res. 2012; 53:1800–1810. [PubMed: 22701043]
31. Cheng D, Meegalla RL, He B, Cromley DA, Billheimer JT, Young PR. Human acyl-CoA:diacylglycerol acyltransferase is a tetrameric protein. Biochem J. 2001; 359:707–714. [PubMed: 11672446]
32. Yu C, Chen J, Lin S, Liu J, Chang CC, Chang TY. Human acyl-CoA:cholesterol acyltransferase-1 is a homotetrameric enzyme in intact cells and in vitro. J Biol Chem. 1999; 274:36139–36145. [PubMed: 10593897]
33. Stone SJ, Levin MC, Farese RV Jr. Membrane topology and identification of key functional amino acid residues of murine acyl-CoA:diacylglycerol acyltransferase-2. J Biol Chem. 2006; 281:40273–40282. [PubMed: 17035227]
34. Wurie HR, Buckett L, Zammit VA. Evidence that diacylglycerol acyltransferase 1 (DGAT1) has dual membrane topology in the endoplasmic reticulum of HepG2 cells. J Biol Chem. 2011; 286:36238–36247. [PubMed: 21846726]
35. Kuerschner L, Moessinger C, Thiele C. Imaging of lipid biosynthesis: how a neutral lipid enters lipid droplets. Traffic. 2008; 9:338–352. [PubMed: 18088320]
36. Windmueller HG, Spaeth AE. Identification of ketone bodies and glutamine as the major respiratory fuels in vivo for postabsorptive rat small intestine. J Biol Chem. 1978; 253:69–76. [PubMed: 618869]
37. Lagakos WS, Gajda AM, Agellon L, Binas B, Choi V, Mandap B, Russnak T, Zhou YX, Storch J. Different functions of intestinal and liver-type fatty acid-binding proteins in intestine and in whole body energy homeostasis. Am J Physiol Gastrointest Liver Physiol. 2011; 300:G803–G814. [PubMed: 21350192]
38. de Vogel-van HM, den Bosch M, de Bunger PJ, Groot H, Bosch-Vermeulen G, Muller Hooiveld M. PPARalpha-mediated effects of dietary lipids on intestinal barrier gene expression. BMC Genomics. 2008; 9:231. [PubMed: 18489776]
39. Mori T, Kondo H, Hase T, Tokimitsu I, Murase T. Dietary fish oil upregulates intestinal lipid metabolism and reduces body weight gain in C57BL/6J mice. J Nutr. 2007; 137:2629–2634. [PubMed: 18029475]
40. Kimura R, Takahashi N, Murota K, Yamada Y, Niiya S, Kanzaki N, Murakami Y, Moriyama T, Goto T, Kawada T. Activation of peroxisome proliferator-activated receptor-alpha (PPAR alpha) suppresses postprandial lipidemia through fatty acid oxidation in enterocytes. Biochem Biophys Res Commun. 2011; 410:1–6. [PubMed: 21640707]

Abbreviations

CM chylomicrons

CARS	coherent anti-Stokes Raman scattering
CLD	cytoplasmic lipid droplets
DLS	dynamic light scattering
DGAT	diacylglycerol acyltransferase
HFD	high-fat diet
TG	triacylglycerol
WT	wild-type

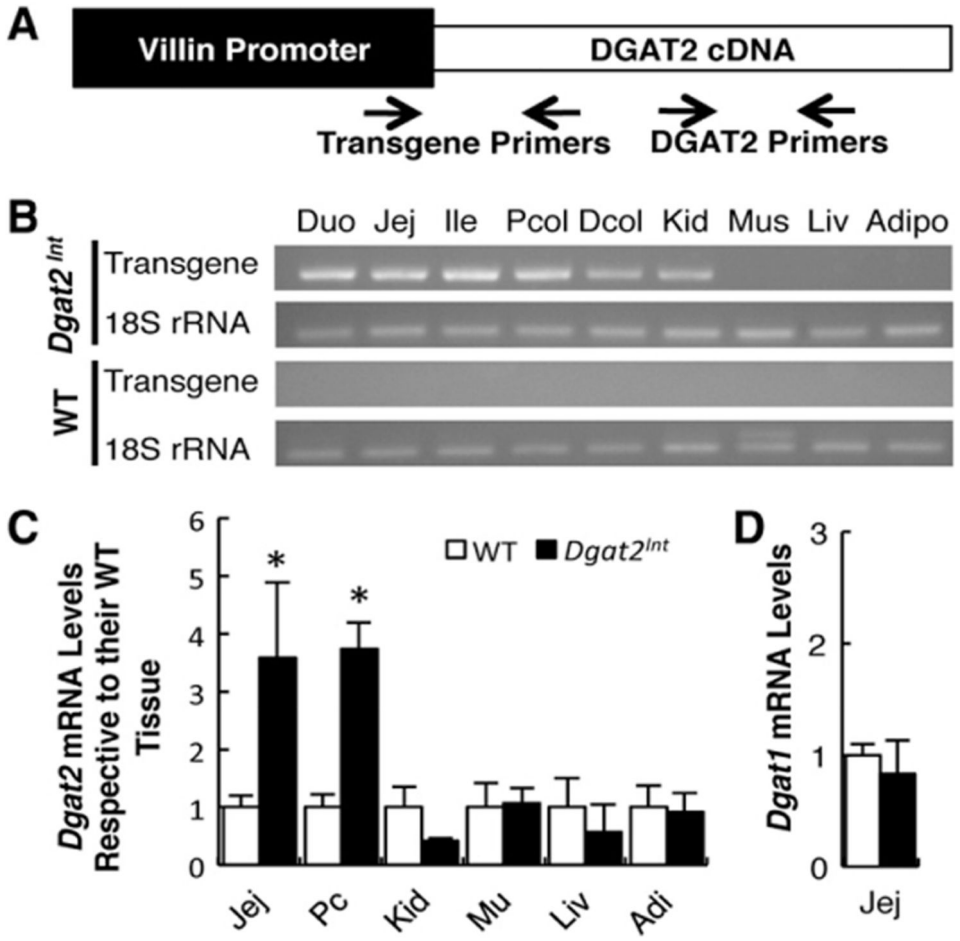

Fig. 1.

Generation of *Dgat2*^{Int} mice. (A) Transgene construct. Mouse *Dgat2* was driven by the villin promoter/enhancer. Primers used for genotyping and transgene detection are highlighted. (B) Tissue-specific *Dgat2* transgene presence. RT-PCR analysis was performed on RNA extracted from the tissues of WT and *Dgat2*^{Int} mice using primers looking for *Dgat2* transgene and 18S rRNA (control). (C) QPCR analysis of *Dgat2* mRNA levels in the jejunum, proximal colon, kidney, muscle, liver and white adipose tissue of *Dgat2*^{Int} compared to WT mice. (D) QPCR analysis of *Dgat1* mRNA level in the jejunum of WT and *Dgat2*^{Int} mice. Abbreviations: duodenum (Duo), jejunum (Jej), ileum (Ile), proximal colon (Pcol), distal colon (Dcol), kidney (Kid), muscle (Mus), liver (Liv), and adipose (Adipo).

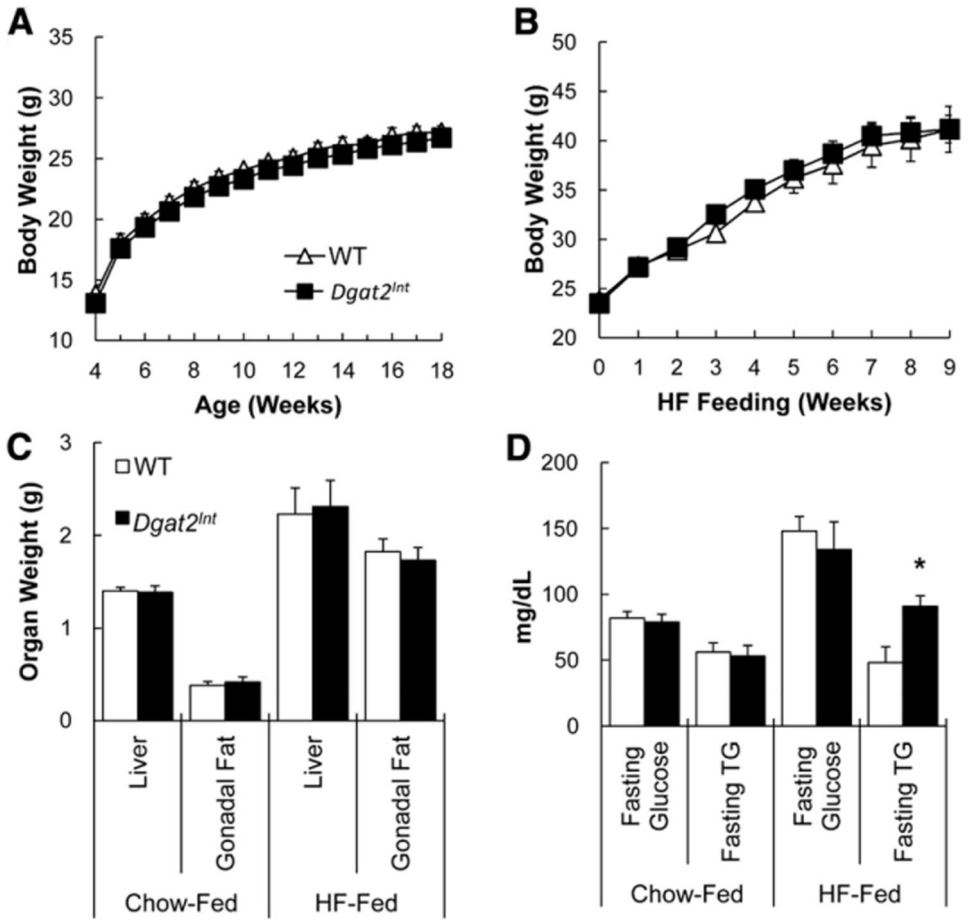

Fig. 2.

Metabolic characteristics of WT and *Dgat2*^{Int} mice fed chow or HFD. (A) Body weights of *Dgat2*^{Int} and WT male mice fed chow diet from weaning to 18 wks of age, n = 12–14 mice. (B) Body weights of *Dgat2*^{Int} and WT male mice fed HFD for 9 wks starting at 10 wks of age, n = 7–11 mice. Body weights were monitored weekly for the duration of the study. (C) Liver and gonadal fat pad weights of *Dgat2*^{Int} and WT male mice fed chow diet from weaning to 18 wks of age or HFD for 9 wks starting at 10 wks of age, n = 12–14 mice and n = 7–11 mice, respectively. Mice were euthanized after a 2-h fast and liver and gonadal fat pad weight was measured. (D) 12 h fasting blood glucose and TG of *Dgat2*^{Int} and WT male mice fed chow diet or HFD for 6 wks, n = 7–8 mice. Asterisk denotes significant difference compared to WT mice (*T-test*), $P < 0.05$.

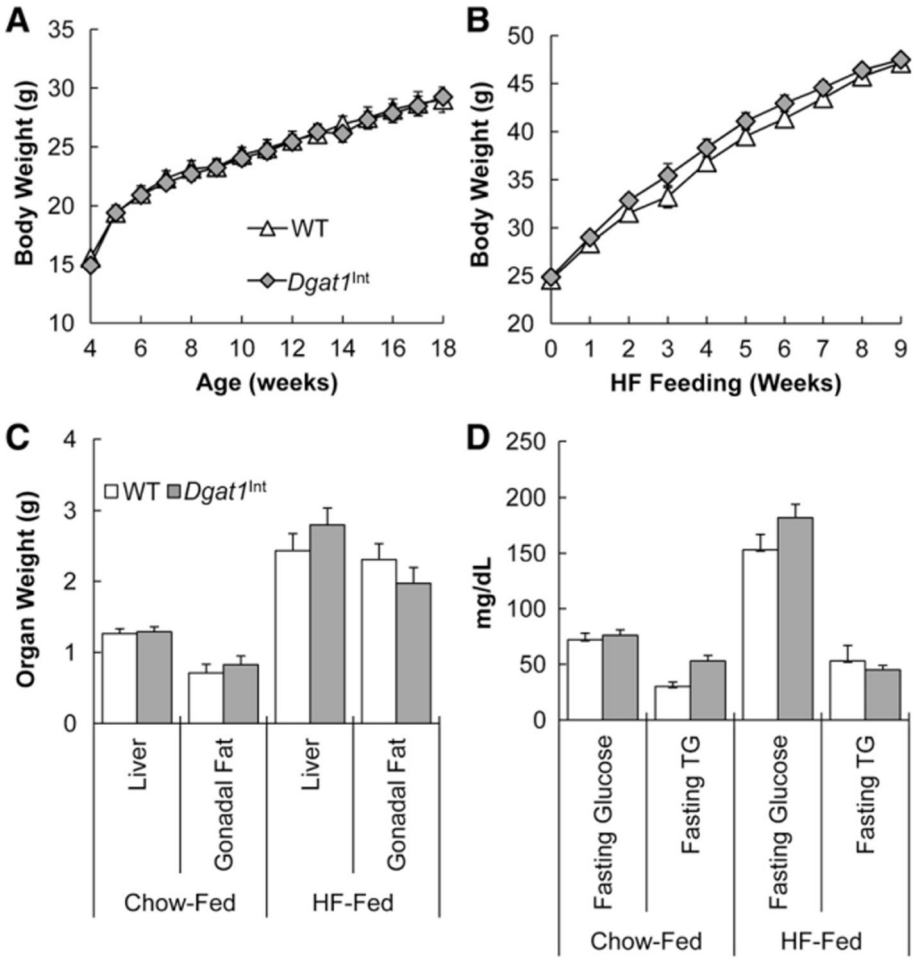

Fig. 3.

Metabolic characteristics of male *Dgat1*^{Int} mice. (A) Body weights of *Dgat1*^{Int} and WT male mice fed a chow diet from weaning to 18 wks of age, n = 9–10 mice. (B) Body weights of *Dgat1*^{Int} and WT male mice fed a HFD for 9 wks starting at 10 wks of age, n = 8–10 mice. Body weights were monitored weekly for the duration of the study. Data are represented as mean ± SEM. (C) Liver and gonadal fat pad weights of *Dgat1*^{Int} and WT male mice on a chow diet from weaning to 18 wks of age or HFD for 9 wks starting at 10 wks of age, n = 9–10 mice and n = 8–10 mice, respectively. Mice were euthanized after a 2 h fast and liver and gonadal fat pad weight was measured. Data are represented as mean ± SEM. (D) Fasting glucose and TG of *Dgat1*^{Int} and WT male mice on a chow diet (16 wks of age) or HFD for 6 to 7 wks, n = 7–8 mice. Mice were fasted for 12 h before measuring fasting glucose and TG concentrations.

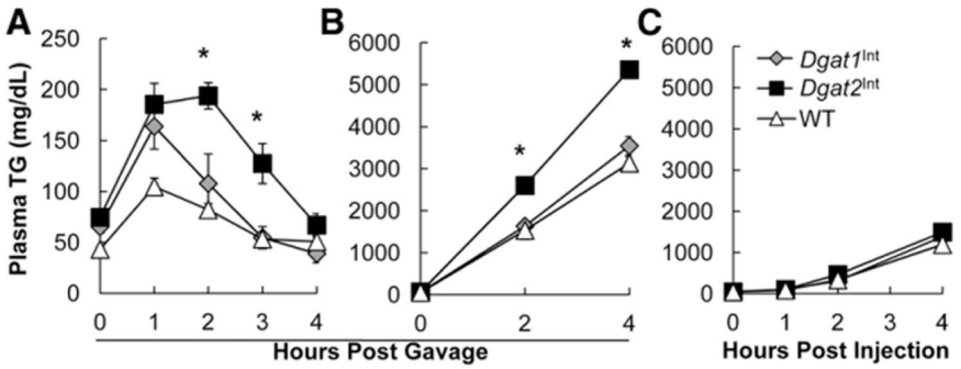

Fig. 4.

Higher postprandial triglyceridemic response and intestinal TG secretion, but similar liver TG secretion, in chow-fed *Dgat2*^{Int} mice compared to *Dgat1*^{Int} and WT mice. (A) Postprandial triglyceridemic response. Plasma TG concentration before and at 1, 2, 3 and 4 h post 200 μl olive oil oral gavage in chow-fed WT, *Dgat1*^{Int} and *Dgat2*^{Int} male mice. Asterisks denote significant difference at time points compared to WT and *Dgat1*^{Int} mice (*one-way ANOVA, Tukey HSD*), $P < 0.05$, n = 7–9 mice. (B) Intestinal TG secretion. Mice were injected IP with 500 mg/kg Tyloxapol to block lipase activity in circulation. After 30 min, mice were given 200 μl olive oil via oral gavage. Plasma TG concentration was measured before, and 2 and 4 h post gavage in chow-fed WT, *Dgat1*^{Int} and *Dgat2*^{Int} male mice. Asterisks denote significant difference at time points compared to WT and *Dgat1*^{Int} mice (*one-way ANOVA, Tukey HSD*), $P < 0.05$, n = 7–11 mice. (C) Liver TG secretion measured. After a 4 h fast, mice were injected IP with 500 mg/kg Tyloxapol to block lipase activity in circulation. Plasma TG concentration was measured before, and 1, 2, and 4 h post injection in chow-fed WT, *Dgat1*^{Int} and *Dgat2*^{Int} male mice, n = 5 mice.

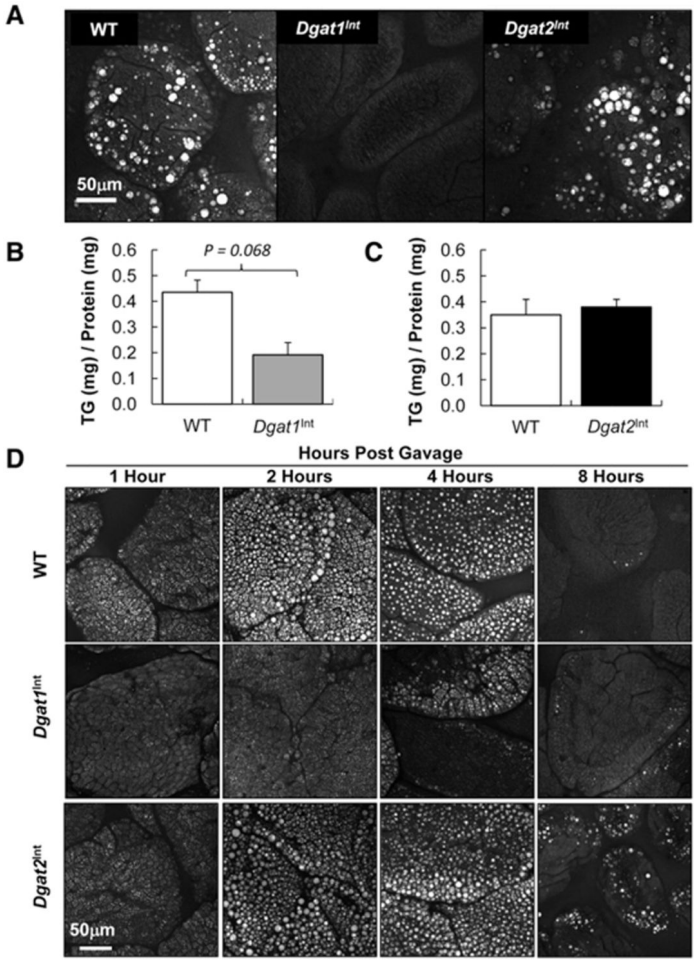

Fig. 5.

TG storage in intestine and liver of chronically and acutely HF challenged WT, *Dgat1*^{Int} and *Dgat2*^{Int} mice. (A) Representative CARS image of TG storage in enterocytes representing the upper jejunum of WT, *Dgat1*^{Int} and *Dgat2*^{Int} mice fed a HFD for 9 wks, after 2 h food removal. (B) TG concentration in intestinal mucosa representing the jejunum of 9 wks HF-fed male *Dgat1*^{Int} male mice and their corresponding WT littermates after 2 h food removal, n = 5 mice. (C) TG concentration in intestinal mucosa representing the jejunum of 9 wks HF-fed *Dgat2*^{Int} and WT male mice after 2 h food removal, n = 6 mice. (D) Representative CARS images of TG storage in CLDs in enterocytes representing the upper jejunum at 1, 2, 4, and 8 h post olive oil gavage in WT, *Dgat1*^{Int} and *Dgat2*^{Int} mice. All mice were fasted 4 h before being administered 200 μl of olive oil via oral gavage.

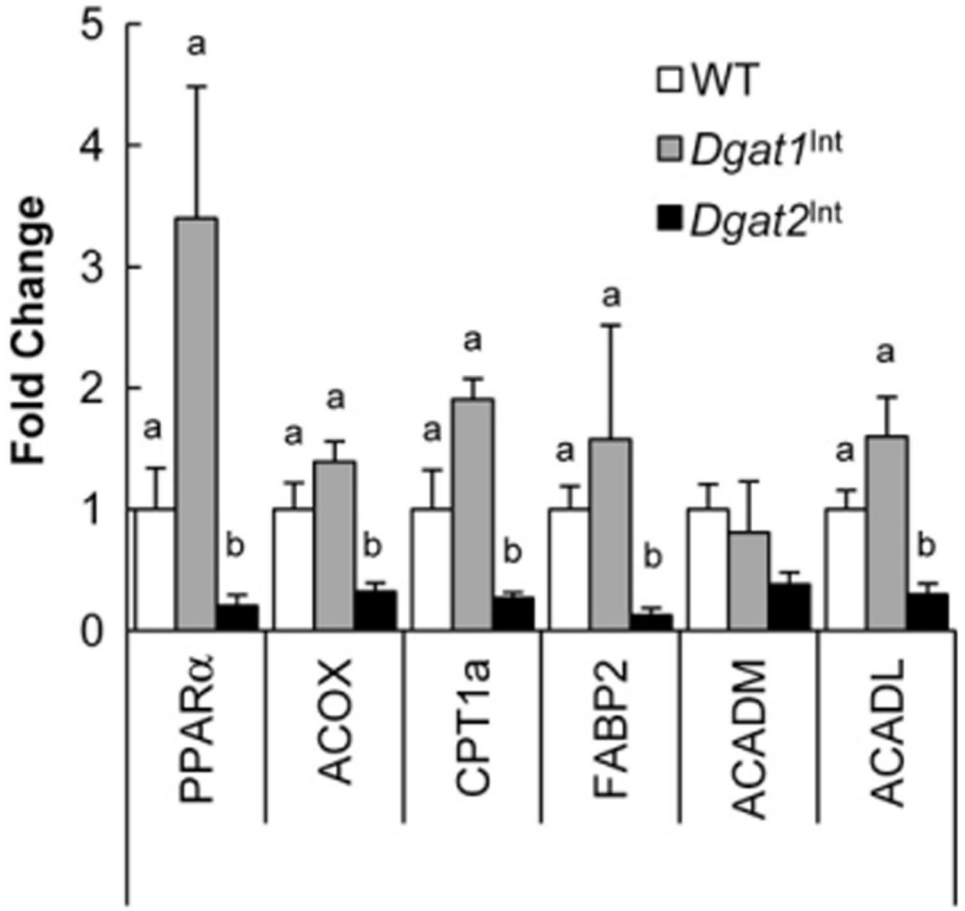

Fig. 6.

Lower mRNA levels for genes involved in fatty acid oxidation in HF-fed *Dgat2*^{Int} compared to *Dgat1*^{Int} and WT mice. QPCR analysis of genes involved in fatty acid oxidation in the jejunum of HFD-fed WT, *Dgat1*^{Int} and *Dgat2*^{Int} male mice after 2 h food removal. Letters denote significant differences between groups relative to each respective gene of WT mice (*one-way ANOVA, Tukey HSD*), $P < 0.05$, n = 4–6 mice.

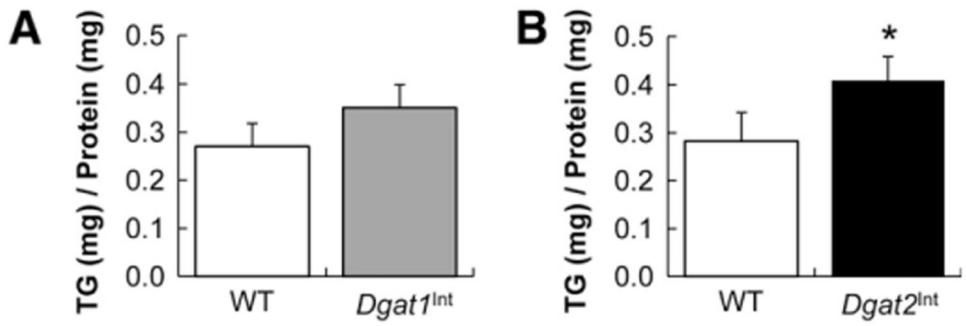

Fig. 7.

Exacerbated hepatic TG storage in HF-fed *Dgat2*^{Int} mice compared to WT mice, but not in *Dgat1*^{Int} mice. (A) TG concentration in the liver of 9 wks HF-fed male *Dgat1*^{Int} male mice and their corresponding WT littermates after 2 h food removal, n = 5 mice. (B) TG concentration in the liver of 9 wks HF-fed *Dgat2*^{Int} and WT male mice after 2 h food removal. Asterisk denotes significant difference compared to WT mice (*T-test*), $P < 0.05$, n = 7–8 mice.

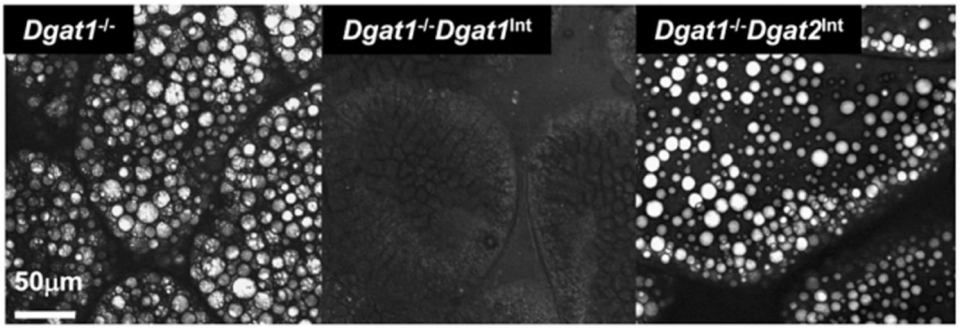

Fig. 8.

TG storage in enterocytes of various transgenic models. (A) Representative CARS images of TG storage in CLDs in enterocytes of the upper jejunum (S2) of *Dgat1*$^{-/-}$, *Dgat1*$^{-/-}$*Dgat1*^{Int} and *Dgat1*$^{-/-}$*Dgat2*^{Int} mice fed a HFD for 9 wks, after 2 h food removal.

Table 1

Primers used for QPCR.

Gene	Primer sequences
18S rRNA	F 5′-TTAGAGTGTTCAAA GCAGGCCCGA-3′
	R 5′-TCTTGGCAAATGCTTTCGCTCTGG-3′
Acadl	F 5′-TTGCTTGGCATCAACATCGCGAG-3′
	R 5′-TGTCATGGCTATGGCACCGATACA-3′
Acadm	F 5′-TCGGTGAAGGAGCAGGTTTCAAGA-3′
	R 5′-AAACTCCTTGGTGCTCCACTAGCA-3′
Acox	F 5′-ATATTTACGTCACGTTTACCCCGG-3′
	R 5′-GGCAGGTCATTCAAGTACGACAC-3′
Cpt1a	F 5′-TGTGGTGTCCAAGTATCTGGCAGT-3′
	R 5′-AACACCATAGCCGTCATCAGCAAC-3′
Dgat1	F 5′-ACCGCGAGTTCTACAGAGATTGGT-3′
	R 5′-ACAGCTGCATTGCCATAGTTCCCT-3′
Dgat2	F 5′-TGGGTCCAGAAGAAGTTCCAGAAGTA-3′
	R 5′-ACCTCAGTCTCTGGAAGGCCAAAT-3′
Fabp2	F 5′-AGAGGAAGCTTGGAGCTCATGACA-3′
	R 5′-TCGCTTGGCCTCAACTCCTTCATA-3′
Pparα	F 5′-TCGCGTACGGCAATGGCTTTATCA-3′
	R 5′-AGCTTTGGGAAGAGGAAGGTGTCA-3′

Table 2

Quantitative dietary fat absorption of HF-fed WT, *Dgat1*^{Int} and *Dgat2*^{Int} mice. Food intake and fecal excretions were determined over 3 days after 6–7 wks of HF feeding. Data are represented as mean ± SEM.

	Food intake g/day (n = 4–5)	Fecal weight g/day (n = 4–5)	Fecal fat % (n = 4–5)
WT	2.3 ± 0.3	0.21 ± 0.02	1.8 ± 0.4
Dgat1^{Int}	2.3 ± 0.1	0.25 ± 0.01	0.8 ± 0.1
Dgat2^{Int}	1.9 ± 0.1	0.24 ± 0.01	1.7 ± 0.2

Table 3

CM size of WT, *Dgat1*^{Int}, *Dgat2*^{Int}, and *Dgat1*$^{-/-}$ mice. CMs isolated from mice 1 h post 200 μl olive oil oral gavage, and measured using DLS. Data are represented as mean ± SEM. Asterisks denote significant difference compared to each other (*one-way ANOVA, Tukey HSD*), $P < 0.05$, n = 5–7 mice.

	Z-average d.nm	Poly-dispersity index	Dominant intensity peak d.nm
WT	115 ± 6	0.25 ± 0.02	153 ± 7
Dgat1^{Int}	114 ± 6	0.25 ± 0.01	156 ± 9
Dgat2^{Int}	124 ± 3	0.24 ± 0.01	167 ± 3
Dgat1$^{-/-}$	58 ± 7*	0.33 ± 0.04	86 ± 9*